RSC Advances

RSC Advances

ARTICLE TYPE

A new pyridoxal based fluorescence chemo-sensor for detection of Zn(II) and its application in bio imaging †

Senjuti Mandal,[a] Yeasin Sikdar,[a] Dilip K. Maiti,[a] Guru Prasad Maiti,[b] Sushil Kumar Mandal,[c] Jayanta Kumar Biswas,[c] Sanchita Goswami[a]*

Abstract: This paper describes the activity of a Schiff base ligand, derived from pyridoxal, as a promising fluorescence probe for biologically important Zn(II) ion sensing. A physiologically compatible pyridoxal based chemosensor **PydDmen** was synthesized and evaluated for its fluorescent response
10 towards metal ions. Chemosensor **PydDmen** exhibits selective turn-on type response in presence of Zn^{2+} in ethanol – water mixture. The addition of EDTA quenches the fluorescence of receptor **PydDmen–Zn^{2+}** complex, making the chemosensor **PydDmen** a reversible one. The response is specific for Zn(II) ions, and remains almost unaffected by the presence of alkali and alkaline earth metals but is suppressed to varying degrees by transition metal ions. The selectivity mechanism of **PydDmen** for Zn^{2+} is the
15 combined effects of proton transfer between the prevailing tautomeric forms, C=N isomerization and CHEF. The DFT optimized structure of the complex is compatible with elemental analysis, mass spectrometry, FT-IR, electronic and NMR spectra. The experimental and theoretical supports in terms NMR spectroscopy and DFT are provided to establish the existence of Zn^{2+} induced transformation of **PydDmen** to a 3-pyridone tautomeric form.

20 Introduction

The zinc ion (Zn^{2+}) is the second most abundant heavy metal ion in the human body and the cellular biochemistry of Zn^{2+} is diverse and far ranging.[1] On the other hand, misregulation of Zn^{2+} is also implicated in human health disorders. It is believed that a
25 lack of zinc ions can result in an increased risk of several diseases such as stature, mental retardation and digestive dysfunction because the majority of biological zinc ions are tightly sequestered by proteins.[2] Additionally, the presence of excess "free zinc" in certain cells may be related to severe neurological disorders such
30 as Alzheimer's and Parkinson's diseases.[3(a),(b)] Therefore, it is necessary to get an insight into the vital roles of Zn^{2+} in biological processes, resulting in great demand regarding the design and development of efficient systems that can selectively and sensitively detect Zn^{2+} in living systems. Several analytical
35 methods have played a vital role in the detection of Zn^{2+} including

UV-Vis-spectroscopy,[3(c)] Potentiometry,[3(d)] flame atomic
50 absorption spectrometry.[3(e)] However, its investigation can be facilitated by the use of fluorescent probes as fluorescence detection, in particular, is considered to be the most effective tool for sensing applications owing to the high sensitivity, easy
55 visualization, short response time for detection and most importantly can be used for real time bio-imaging.[4] Unfortunately, zinc ions are not intrinsically fluorescent, making direct quantitative detection a difficult task.[5,6] A variety of fluorescent sensors for Zn^{2+} have been reported based on various
60 fluorophores.[7-9] Continuous effort has been dedicated improving the effectiveness of Zn^{2+} sensors.

We are mainly concerned with Schiff bases as probes because Schiff bases are suitable ligands for metal ions. Schiff bases are inherently non-/poorly fluorescent due to conventional modes of
65 non-radiative decay pathways such as, isomerisation of C=N bond in the excited state and ESIPT involving phenolic proton.[10,11] Therefore, it is reasonable to expect that if we limit to simple Schiff bases as prospective probes for metal cations, the probable signaling pathways involve restriction of C=N isomerisation,
70 ESIPT and CHEF (Scheme 1). But, Schiff base related probes can also coordinate strongly other physiologically available metal ions. Therefore, new strategies should be developed to improve Zn^{2+} selectivity of the probe. In order to make analyte binding more specific and favourable, it would be desirable if the binding
75 pattern of the probe with the analyte is unique, i.e. the probe is

a Department of Chemistry, University of Calcutta, 92, A. P. C. Road, Kolkata – 700009, India. E-mail: sgchem@caluniv.ac.in
b Department of Molecular Biology and Biotechnology, University of
40 *Kalyani, Kalyani-741235, West Bengal, India.*
c Department of Ecological Engineering & Environmental Management, University of Kalyani, Kalyani, Nadia-741235, West Bengal, India.
†Electronic Supplementary Information (ESI) available:[NMR & IR of the ligand, IR & ESI-MS of the Complex, Job's plot, EDTA reversibility plot,
45 detection limit plot, table of fluorescence lifetime of ligand and complex, tale of theoretical bond length and bond angle of complex, table of energy of selected molecular orbitals of complex, tables for calculated vertical electronic transitions of complex]. See DOI: 10.1039/b000000x/

transformed after binding to the analyte of choice. Such type of phenomena enhances the selectivity manifolds. Tautomerization is an efficient transformable factor in such cases.[12] Spring and co-workers have beautifully and efficiently exploited the imidic acid and amide tautomeric forms for selective binding with metal ions.[12] Till date, reports on tautomerism during analyte binding is relatively scarce in the literature (Chart 1†).[13]
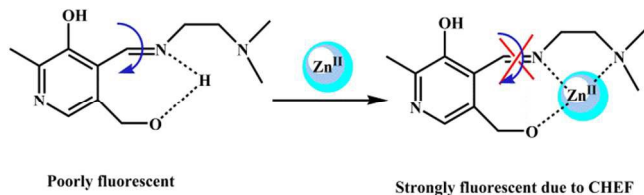
Scheme 1: Probable signaling pathways of probe **PydDmen**.

In order to enhance the bio-compatibility in bioimaging, we have already started working with pyridoxal[14] containing Schiff bases as chemosensors and reported a chemosensor that selectively detects Cu^{2+} ion.[14,15] The pyridoxal and its derivatives exhibit a wide range biological properties and have been used as substrates in many biological transformations.[16-21] In order to explore further this less ventured path, we herein constructed a novel turn-on sensor for Zn^{2+}, which can exhibit emission at longer wavelength (483 nm). The 3-hydroxy pyridine moiety present in the probe permits 3-hydroxy pyridine – 3-pyridone tautomeric equilibrium to exist.[22] The spectroscopic behaviour of Schiff base and **PydDmen** [((2-(dimethylamino)ethylimino)methyl)-5-(hydroxymethyl)-2-methylpyridin-3-ol] shows that it is an excellent chemosensor for Zn^{2+} in ethanol-water and can be used for Zn^{2+} monitoring in living cells. The NMR spectroscopy and DFT study are utilized to establish the Zn^{2+} induced transformation of **PydDmen** to 3-pyridone tautomeric form in solution. To the best of our knowledge, this is the first report that establishes such type of tautomeric transformation as mechanistic rationale by means of ^{1}H NMR, ^{13}C NMR and ^{13}C DEPT methods.

Results and discussion

Synthesis and FTIR spectral characterization of PydDmen

The chemosensor **PydDmen** has been synthesized by condensing pyridoxal hydrochloride with N,N-dimethylethylenediamine under refluxing conditions in ethanol medium (Scheme 2) and the structure of **PydDmen** was well characterized by ^{1}H NMR and FTIR spectroscopy (Fig. S1†). The **PydDmen-Zn^{2+}** complex was characterized by recording FTIR and ESI-MS spectra (Fig. S2†).

FTIR spectra of **PydDmen** showed the characteristic band due to ν(C=N) at 1650 cm^{-1}. In the Zn^{2+} complex, the ν(C=N) absorption appears at lower energy (ca. 1631cm^{-1}) indicating possible coordination to the metal center. The complexes also display broad band of medium intensity around 3400 cm^{-1} attributable to the -OH stretching vibration of the –CH$_2$OH group of the pyridoxal part of the chemosensor **PydDmen**.[23]
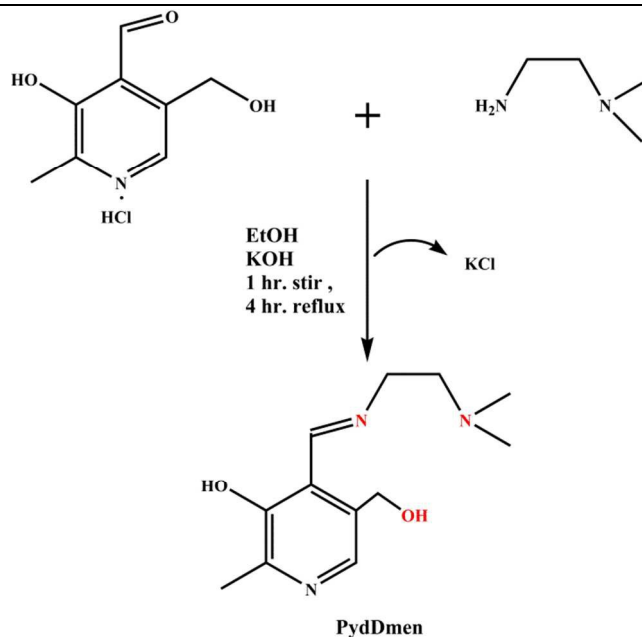
Scheme 2: Preparation of chemosensor **PydDmen**.

UV-Vis spectroscopic investigation of PydDmen

In order to ascertain the complexation of Zn^{2+} by **PydDmen**, absorption titrations were carried out by adding varied concentrations of $Zn(NO_3)_2.2H_2O$ to a fixed concentration of **PydDmen**. Fig. 1 depicts spectrophotometric changes upon titrating a fixed concentration of **PydDmen** (5×10^{-5} M) with incremental additions of $Zn(NO_3)_2$ (55×10^{-5} M) in EtOH/H$_2$O (4:1, v/v, 25 mM Tris buffer, pH 7.4). The absorption spectrum of **PydDmen** in same solvent displayed sharp absorption bands centered at 253 nm and 335 nm, which are assigned to the π–π* transitions. The absorption bands at 415 nm is attributed to the n–π* transitions of azomethine group.
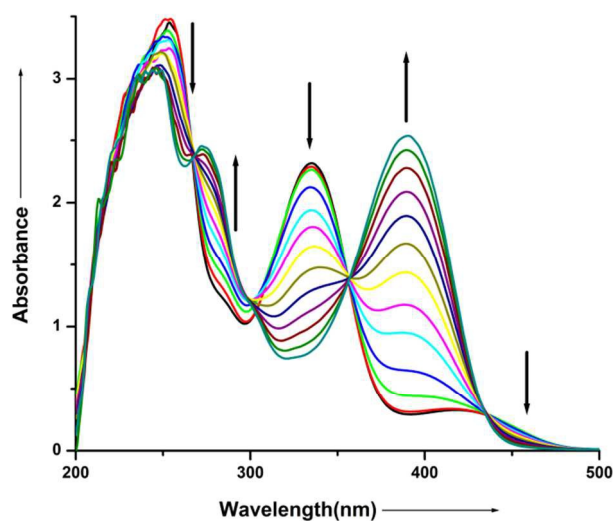
Fig. 1 UV-Vis spectral changes of sensor **PydDmen** (c =5 x 10^{-5} M) in EtOH/H$_2$O (4:1, v/v, 25 mM Tris buffer, pH 7.4) solutions upon addition of Zn^{2+} ions (0-55 equivalent) (c = 0-55 x 10^{-5} M) in EtOH/ H$_2$O (4:1, v/v) at pH 7.4.

However, addition of Zn^{2+} induced dramatic modification both in the maxima and shape of the said bands of **PydDmen**. The band at 253 nm is decreased slightly, accompanied by a blue shift to 246 nm. The band maxima at 335 nm is gradually decreased 5 and a new band appeared at 295 nm. Another broad and moderately intense band around 390 nm could be assigned to O^- (phenolate) $\leftrightarrow Zn^{2+}$ (LMCT or MLCT). These spectral changes, spanning the 240-390 cm^{-1} region, are indicative of Zn^{2+} coordination induced perturbation of the - $(OH)C = C - C = N -$ 10 portion of the ligand during the course of the reaction.[24] Therefore, these absorption peaks were expected to correspond to coordination of **PydDmen** with Zn^{2+} generating the **PydDmen-Zn^{2+}** coordinated species. The accompanying isosbestic points at 268, 302, 356 and 435 nm clearly indicate that the transition 15 between the free and the complexed species occurs and a stable complex resulted at a certain composition. The stoichiometry of the complex formed between **PydDmen** and Zn^{2+} is 1:1 based on Job's plot (Fig. S3†).

20 Binding behaviour analysed by fluorescence spectroscopy

The chemosensor **PydDmen** is poorly fluorescent in nature when excited at 411 nm in $EtOH/H_2O$ (4:1, v/v, 25 mM Tris buffer, pH 7.4), which may be attributed to the combined effect of C=N isomerisation and ESIPT as commonly encountered in Schiff 25 bases.[10] The fluorescence sensing behaviour of **PydDmen** towards Zn^{2+} was investigated in buffer solution at physiological pH in $EtOH/H_2O$ (4:1, v/v, 25 mM Tris buffer, pH 7.4) using a 5 x 10^{-6} M solution (Fig. 2). $Zn(NO_3)_2$ was chosen as the representative Zn^{2+} species in the following experiment. Upon addition of 14 30 equivalents of $Zn(NO_3)_2$, an enhancement in fluorescence spectrum was observed at 483 nm and maximum emissive wavelength shifts from 477 to 483 nm.
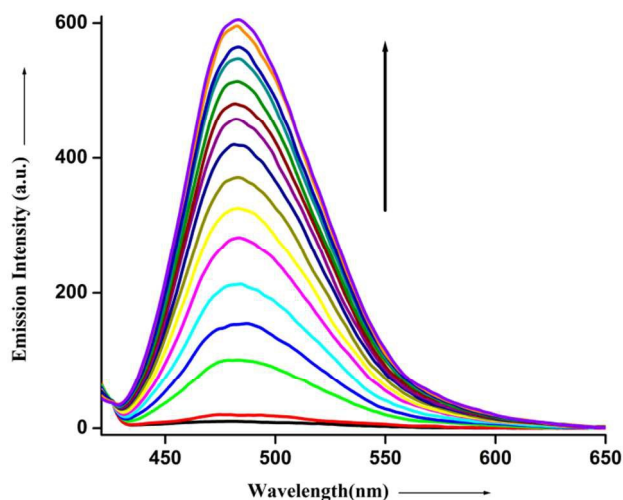
35 **Fig. 2** Fluorescence emission changes of **PydDmen** (c = 5× 10^{-6} M) upon addition of Zn^{2+} ions (c = 0-70× 10^{-6} M) in EtOH/ H_2O (4:1, v/v) in tris buffer at pH 7.4 (λ_{ex}=411 nm).

Under the same conditions, the selective sensing behaviour of **PydDmen** was validated using a variety of other metal ions in 40 place of Zn^{2+}, viz., Li^+, Na^+, K^+, Sr^{2+}, Ba^{2+}, Ca^{2+}, Cr^{3+}, Mn^{2+}, Fe^{2+},

Co^{2+}, Ni^{2+}, Cu^{2+}, Hg^{2+}, Pb^{2+} and Al^{3+}. But they do not show any significant change of fluorescence intensity of **PydDmen**, whereas Mg^{2+} and Cd^{2+} produce moderate enhancements (Fig. 3). From Fig. 3 it is clear that the Zn^{2+} ion gives rise to the largest 45 fluorescence enhancement among these metal cations.
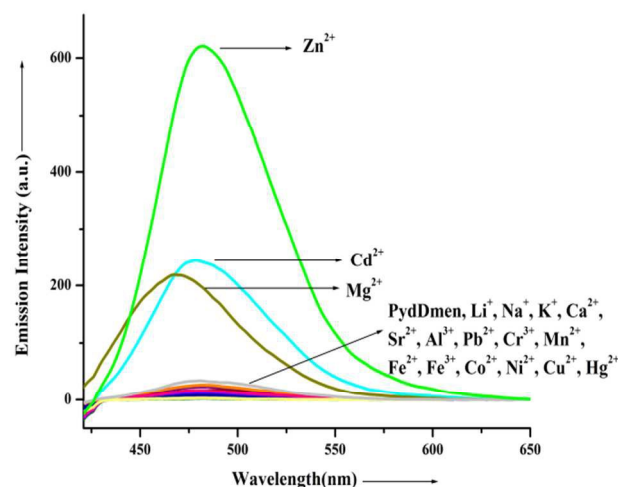
Fig. 3 Emission spectra of **PydDmen** (c=5x10^{-6} M) in presence of Zn^{2+}, Li^+, Na^+, K^+, Ca^{2+}, Sr^{2+}, Al^{3+}, Pb^{2+}, Cr^{3+}, Mn^{2+}, Fe^{2+},Fe^{3+}, Co^{2+}, Ni^{2+}, Cu^{2+}, Cd^{2+}, Hg^{2+} and Mg^{2+}(c=70x10^{-6} M each metal ion) in $EtOH/H_2O$ (4:1, v/v, 50 25 mM Tris buffer, pH 7.4) (λ_{ex}=411 nm).

The competitive studies of **PydDmen** towards Zn^{2+} over other metal ions are carried out by adding 14 equivalents of Zn^{2+} to the solution of **PydDmen** (5 x 10^{-6} M) in the presence of 14 equivalents of other metal ions, viz., Li^+, Na^+, K^+, Sr^{2+}, Ba^{2+}, Ca^{2+}, 55 Cr^{3+}, Mn^{2+}, Fe^{2+}, Fe^{3+}, Co^{2+}, Ni^{2+}, Cu^{2+}, Hg^{2+}, Pb^{2+}, Al^{3+}, Mg^{2+} and Cd^{2+}. The competition experiments showed that the emission profile of the **PydDmen-Zn^{2+}** complex is more or less unaffected in the presence of other cations (Fig. S4†).

Titration of **PydDmen** with Zn^{2+} (concentration increased 60 from 0 - 70 μM) revealed enhancement (up to 52 fold enhancement) of fluorescence intensity at 483 nm as a function of the added Zn^{2+} concentration (Fig. 2), suggesting a sensitive and selective recognition of Zn^{2+} by **PydDmen**. The chelation of Zn^{2+} by **PydDmen** occurs *via* $N_{amine/imine}$ and O_{alkoxo} giving rigidity to 65 the binding core. Therefore, C=N isomerisation as well as ESIPT is inhibited, reducing the non-radiative decay processes and increasing the possibility of fluorescence emission. This phenomenon results in chelation enhanced fluorescence (CHEF).

The linear relationship of the fluorescence titration showed 70 that **PydDmen** responded to Zn^{2+} in 1:1 stoichiometry as evident from the Job's plot from absorption studies (Fig. S3†). The association constant for Zn^{2+} was estimated to be 1.18 x 10^4 M^{-1} by the linear Benesi-Hildebrand equation $F_0/(F - F_0) = F_0/[$**PydDmen**$] + F_0/[$**PydDmen**$] \times K_a \times [Zn^{2+}]$. F is the change in the 75 fluorescence intensity at 483 nm, K_a is the association constant, and [**PydDmen**] and [Zn^{2+}] are the concentration of **PydDmen** and Zn^{2+} respectively. By plotting $F_0/(F - F_0)$ against the reciprocal of the concentration of Zn^{2+}, the association constant value K_a is obtained from the ratio intercept/slope with a good 80 linear correlation coefficient ($R^2 = 0.998$) (Fig. 4).
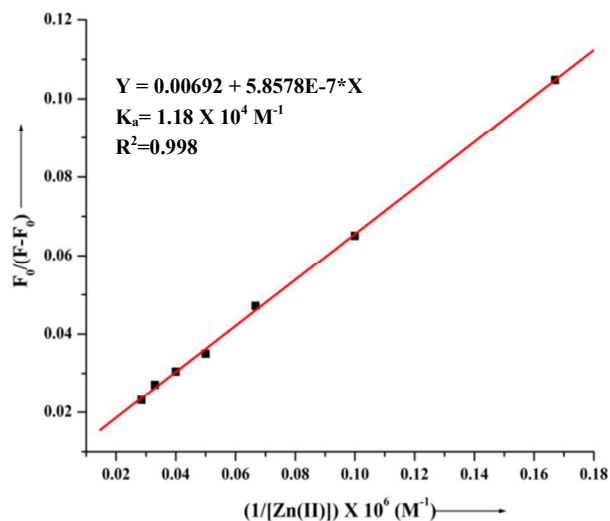
Fig. 4 Benesi-Hildebrand expression fitting of fluorescence titration curve of **PydDmen** (c = 5× 10-6 M) upon addition of Zn2+ ions (c = 6, 10, 15, 20, 25, 30 and 35× 10-6 M) in EtOH/ H2O (4:1, v/v) in tris buffer at pH 7.4 (λex=411 nm).

Since many fluorescent probes are sensitive to pH, it is necessary to investigate the pH effect to find the optimal condition when the fluorescence measurements are to be carried out. From the pH dependence of fluorescence study (Fig. S5†), it was found that the fluorescence intensity of **PydDmen** at 483 nm in EtOH/H$_2$O remains unaffected at pH 7.4 which makes it suitable for application under physiological conditions. These results indicate that **PydDmen** can be used as a selective fluorescent probe to recognize and distinguish Zn^{2+} in the presence of various metal ions at pH 7.4.

We have also performed a reversibility experiment (Fig. S6†) which proved that the binding of Zn^{2+} to **PydDmen** is reversible which is the key requirement of an ideal biologically relevant chemosensor because binding of guest molecule must occur reversibly. In the presence of Na$_2$EDTA, a strong chelating ligand, due to its strong affinity towards Zn^{2+}, decomposition of the **PydDmen-Zn^{2+}** entity takes place thereby reproducing non fluorescent **PydDmen**. As shown in Fig. S6† after the addition of Na$_2$EDTA, the emission intensity of the original ligand was gradually lost. This phenomena certainly gives a tacit support towards the reversible binding of **PydDmen** with Zn^{2+}.

To determine the detection limit, following equation was used. DL= K x Sb/S where K = 2 or 3 (we take 3 in this case), Sb is the standard deviation of the blank solution and S is the slope of the calibration curve.[25] Here, the detection limit of **PydDmen** (Fig. S7†) as a chemosensor for Zn^{2+} was found to be 40.78 x 10^{-7} M which is sufficiently low for the detection of submillimolar concentrations of Zn^{2+} ions found in many chemical systems.[26]

The fluorescence quantum yields (Φ$_f$)[27] of **PydDmen** and **PydDmen-Zn^{2+}** states were found to be 0.094 and 0.408 respectively (Table S1†). This substantial increase in the quantum yield of **PydDmen** in the presence of Zn^{2+} advocates its credibility as an efficient Zn^{2+} sensor.

We have also examined the anion independency of **PydDmen** by using Cl$^-$, Br$^-$, I$^-$, NO$_3^-$, CH$_3$COO$^-$, ClO$_4^-$ salts and the spectral output is represented in Fig. S8†.

Time resolved measurement

A picosecond time-resolved fluorescence technique has been used to examine the decay process of free sensor **PydDmen** and **PydDmen-Zn^{2+}** in EtOH/H$_2$O (4:1, v/v, 25 mM Tris buffer, pH 7.4, 298 K). According to the equations $\tau^{-1} = k_r + k_{nr}$ and $k_r = \Phi_f/\tau$, the radiative decay rate constant k_r and the total nonradiative decay rate constant k_{nr} of **PydDmen** and Zn^{2+}-bound species were calculated. The decay curve of the fluorescence intensity of **PydDmen** and fitting data were shown in Fig. 5 and Table S1†.
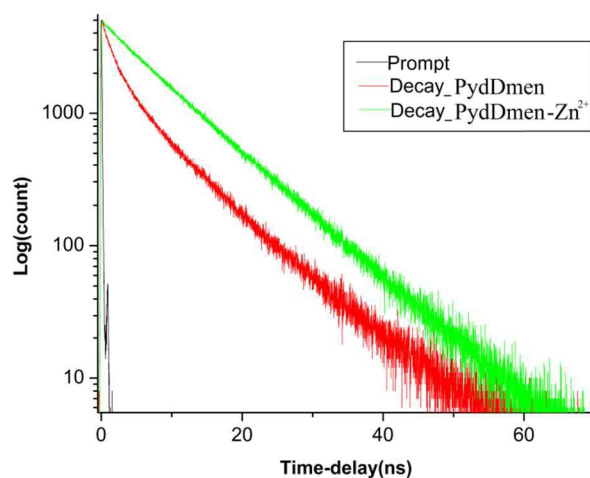
Fig. 5 Time resolved fluorescence decay of sensor **PydDmen** (red) and **PydDmen-Zn^{2+}** (green) and prompt (black) (λ$_{ex}$=375nm).

The decay curve and fitting data of **PydDmen** suggested that there were three main isomeric components of **PydDmen** to absorb light and emit fluorescence photons of lifetime at 0.821 ns, 3.375 ns and 9.334 ns. The average fluorescence lifetime (τ) of **PydDmen** was estimated as 3.79 ns. The radiative and nonradiative decay rate constants are calculated to be 2.48 x 10^7 and 2.39 x 10^8 sec^{-1} respectively indicating that the nonradiative decay is the predominant process in the excited states.[28] In the presence of 70 x 10^{-6} M Zn^{2+}, the time-resolved fluorescence decay showed significant change, which indicated two components corresponding to **PydDmen-Zn^{2+}** at 9.078 ns and a small number of isomeric components of **PydDmen** at 1.479 ns. The lifetime is increased to 8.23 ns, which is longer than that of the free-**PydDmen**. The radiative and nonradiative decay rate constants changed to 4.96 x 10^7 and 7.19 x 10^7 s^{-1} respectively. This result suggested that both the radiative and nonradiative decay processes became comparative resulting in a strong fluorescence.

^{1}H and ^{13}C NMR titrations and mode of binding present in the 3-pyridone tautomeric form

In order to evaluate the binding mode of **PydDmen** with Zn^{2+}, ^{1}H and ^{13}C NMR titrations, and ^{13}C-DEPT NMR experiment were performed by gradual addition of Zn(CH$_3$COO)$_2$.2H$_2$O to the DMSO-d$_6$ solution of **PydDmen**. ^{1}H NMR spectroscopy revealed significant differences as shown in Fig. 6 in the chemical shifts of **PydDmen** and **PydDmen-Zn^{2+}**, which could be applied for establishing the structure of **PydDmen-Zn^{2+}**. As presumed from the UV-Vis study (Scheme 3), the - (OH)C = C – C = N – region of **PydDmen** is severely perturbed after addition of Zn^{2+}.

Therefore, it may be speculated that addition of Zn^{2+} induces a transformation to **PydDmen**. Again, it is well documented that 3-hydroxy pyridine-bearing moieties could undergo tautomerism producing the 3-pyridones.[15] If this speculation is true, (Scheme 4), then, it is expected that H_a, H_b, H_d and H_e protons would be upfield shifted because of through bond propagation effect due to tautomerism. Given the greater distance from the perturbed zone, only small differences in the chemical shift values for H_e and H_b are expected. Due to conversion of N_{imine} to N_{amine}, H_g would undergo moderate upfield shift. For the H_h protons, downfield shift is expected as the NMe_2 lone pair is used up in the complexation process.

PydDmen

PydDmen-Zn^{2+}
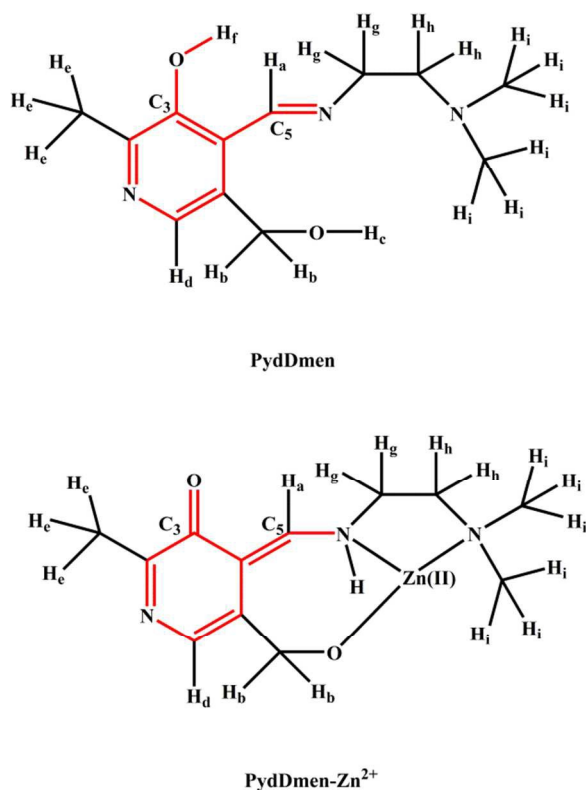
Scheme 3: Zn^{2+} induced tautomerism in **PydDmen** (red color indicate the change in molecular fragment due to Zn^{2+} binding).
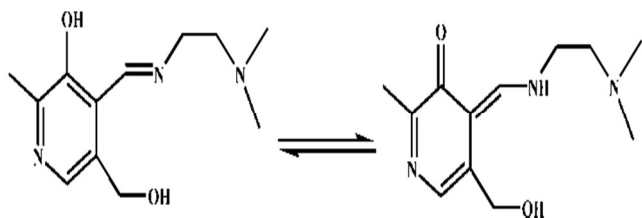
Scheme 4: Pathway of tautomerism in **PydDmen**

Analysis of the ^{1}H NMR spectra after titration revealed that the speculated output were in good agreement with the experiment (Fig. 6). Upon addition of 0.5 equivalent of Zn^{2+} to a solution of **PydDmen**, the signals for H_a, H_d, H_b, H_g, H_h and H_e significantly broadened indicating incomplete complexation between **PydDmen** and Zn^{2+}. After the addition of one equivalent of Zn^{2+},
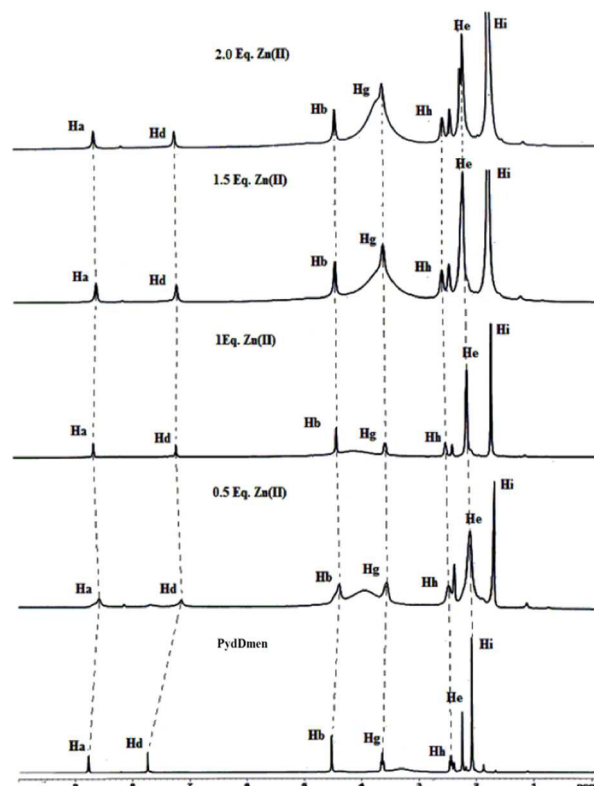
Fig. 6 ^{1}H NMR titration experiment of **PydDmen** with Zn^{2+}.

the resonances of H_a, H_b, H_d, H_e, H_g protons were found to be shielded relative to resonances for **PydDmen** indicating enhancement of electron density in the associated regions (Table S2†). Deprotonation of –CH_2OH group due to coordination to Zn^{2+}, would accumulate negative charge on the oxygen atom resulting in an upfield shift for H_b. But, subsequent complexation process decreases electron density on H_b. Therefore, the extent of upfield shift is less for H_b. The same logic holds true for H_g protons also. The resonances of methylenic protons H_h, α to -NMe_2 fragment, were deshielded and show downfield shift from 2.47 ppm to 2.53 ppm. To understand the fate of the C_3-O_1H_f, a ^{13}C NMR experiment was executed (Fig. 7). A new peak appeared at δ 174.0, which was disappeared in the ^{13}C-DEPT experiment (Fig. 4). It confirms that C_3-O_1H_f was transformed to corresponding ketone. The ligand after complexation with zinc transformed to corresponding 3-pyridone-Zn^{2+} complex i.e. **PydDmen-Zn^{2+}** (Scheme 3). The imine bond was subsequently transformed to an amino exocyclic double bond (C_5), which appeared at δ 166.1. There were no further changes when more than one equivalent of Zn^{2+} were added, which was indicative of the 1 : 1 binding ratio between the sensor and Zn^{2+}. These features are in accordance with the hypothesis that Zn^{2+}-induced tautomerisation of the **PydDmen** occurs and coordinating environment of Zn^{2+} is composed of two N_{amine} and one O_{alkoxo} of the **PydDmen**. Moreover, the reaction mechanism was also confirmed by mass spectral analysis, and a peak at *m/z* 386.08 is

assignable to the mass of [**PydDmen** - Me + Zn^{2+} + H_2O + CH_3COO^-].
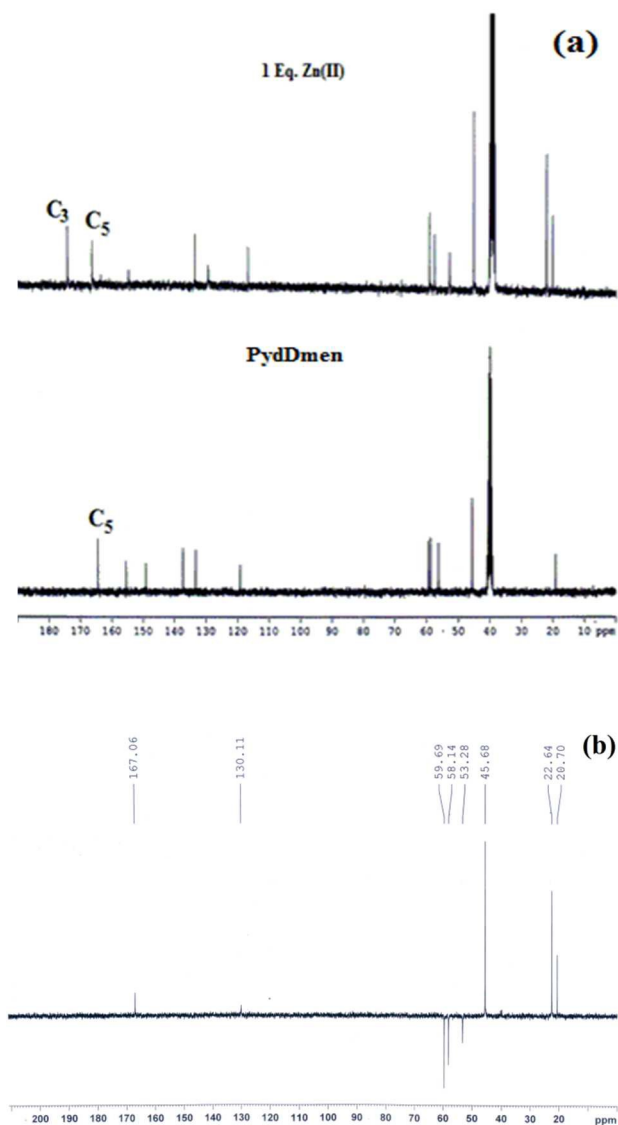
Fig. 7 (a) ^{13}C NMR of **PydDmen** and **PydDmen-Zn^{2+}** in DMSO-d$_6$. (b) ^{13}C DEPT spectral output after adding 1 equivalent of Zn^{2+} in **PydDmen** in DMSO-d$_6$.

To further reinforce the Schiff base transformation phenomena and mode of complexation between **PydDmen** and Zn^{2+}, DFT calculations were carried out. Since attempts to isolate single crystals of **PydDmen-Zn^{2+}** suitable for X-ray diffraction analysis were unsuccessful, the optimized structure of the complex was computed by theoretical methods. The ground state structures of **PydDmen** and **PydDmen-Zn^{2+}** were optimized by density functional theory (DFT) as implemented in the Gaussian 09 (B3LYP/6-311G(d,p)) software package.[29] Full geometry optimizations were carried out at the UB3LYP level for **PydDmen** and **PydDmen-Zn^{2+}**, which are shown in Fig. 8.
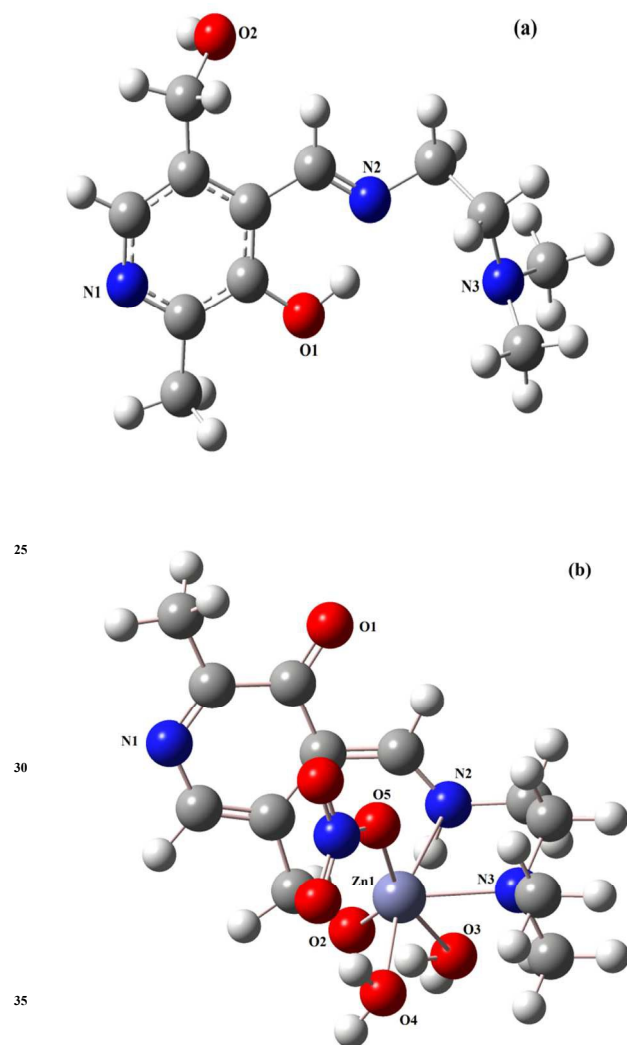
Fig. 8 B3LYP optimized structure of (a) **PydDmen** and (b) **PydDmen-Zn^{2+}**.

In the optimized structure of **PydDmen-Zn^{2+}**, it is clear that **PydDmen** is present in its pyridone tautomeric form and Zn^{2+} is coordinated by means of two N_{amine} atoms and one O_{alkoxo} atom. One nitrate anion and two water molecules complete the six coordination geometry around Zn^{2+}. The optimized bond parameters are given in Table S3†. Energy of different molecular orbitals of **PydDmen-Zn^{2+}** were calculated and given in Table S4†. Contour plots of some selected molecular orbitals of **PydDmen-Zn^{2+}** are given in Fig. S9†. The spatial distributions of Highest Occupied Molecular Orbital (HOMO) and the Lowest Unoccupied Molecular Orbital (LUMO) of **PydDmen** and **PydDmen-Zn^{2+}** are presented in Fig. 9. The energy gaps between HOMO and LUMO in **PydDmen** and **PydDmen-Zn^{2+}** were 3.80 eV and 3.28 eV respectively. The UV-Vis absorption spectra of **PydDmen-Zn^{2+}** were calculated with electronic ground and excited states through time dependent density functional theory calculations (TDDFT) using conductor-like polarizable continuum model (CPCM) in ethanol. The calculated singlet–singlet vertical electronic transitions are summarized in Table S5†. The calculated electronic transitions are very close to the experimental electronic

bands. All the transitions in **PydDmen-Zn²⁺** have intra-ligand charge transfer (ILCT) origin.
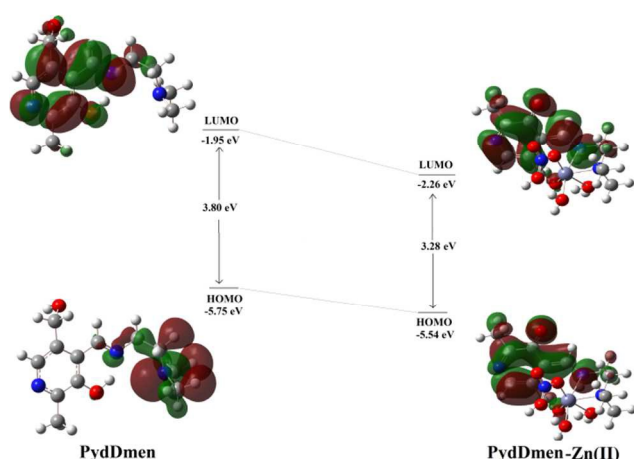
Fig. 9 HOMO and LUMO distribution of **PydDmen** and **PydDmen -Zn²⁺**.

₅ **Biological implications of PydDmen**

To demonstrate the potential application of **PydDmen**, the intracellular Zn²⁺ imaging behaviour of **PydDmen** was studied on A549, human lung cancer cell lines by fluorescence microscopy. After incubation with **PydDmen** (10 μM) at 37ºC for 10 min, the ₁₀ cells displayed no intracellular fluorescence (Fig. 10(B)). However, cells displayed light fluorescence with the addition of low concentration of zinc ions (1μM) (Fig. 10(C)) and exhibited gradually intensive fluorescence when exogenous Zn²⁺ was introduced into the cell via incubation with a zinc nitrate salt ₁₅ solution (Fig. 10(D)-(F)). The intensive fluorescence behaviour was, however, strongly suppressed when TPEN (100μM) was added to the medium. Since TPEN confers having a strong scavenging action on Zn²⁺ ions, the sensors were competitively inhibited to bind with Zn²⁺ ions, as a result, the intensive ₂₀ fluorescence disappeared (Fig. 10(H)). This presents the confirmatory evidence of the sensor having the selectivity to sense Zn²⁺ ions. The fluorescence responses of **PydDmen** with various concentrations of added Zn²⁺ proves that such fluorescence intensity can be used as indelible signature of selective sensor ₂₅ response clearly evident from the cellular imaging. Hence, these results indicate that **PydDmen** is an efficient candidate for monitoring changes in the intracellular Zn²⁺ concentration under biological conditions.

The cytotoxicity study (MTT assay) in human lung cancer ₃₀ cells treated with various concentrations of **PydDmen** for up to 12 h as shown in Fig. 11 showed that **PydDmen** concentrations up to 10μM did not show significant cytotoxic effects on human lung cancer cells for at least up to 12 h of its treatment. The study suggests that **PydDmen** can be readily used as an efficient, ₃₅ selective and sensitive tool for bioimaging at the indicated doses and incubation time without cytotoxic effects. Thus the intensity based Zn-sensors can offer promising potential to probe physiological and biochemical consequences of metal dynamics with wide metabolic spectrum in cellular environment with ₄₀ appreciable fidelity.
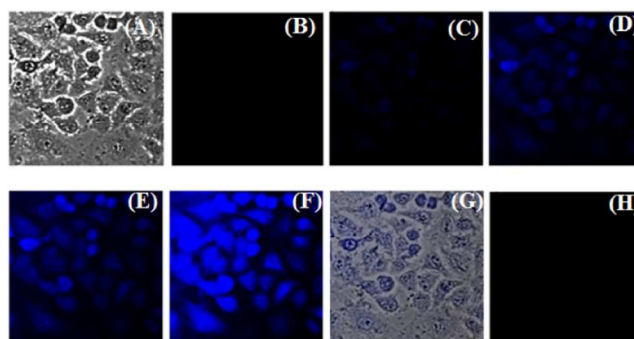
Fig. 10 (A) Phase contrast, (B) fluorescence image of A549 cells incubated with 10μM **PydDmen** for 10 min at 37ºC. **PydDmen** (10μM) incubated cells were washed with PBS and were exposed to the presence ₄₅ of sequentially increased concentrations of added extracellular Zn²⁺ ion as (C) 1μM, (D) 10μM, (E) 20μM and (F) 50μM (G) Represent the merge image of phase contrast and fluorescence image. (H) Represent disappearance of fluorescence intensity in the A549 cells treated with the **PydDmen** and Zn²⁺ ion after further addition of 100μM TPEN. For all ₅₀ imaging, the samples were excited at 410 nm.
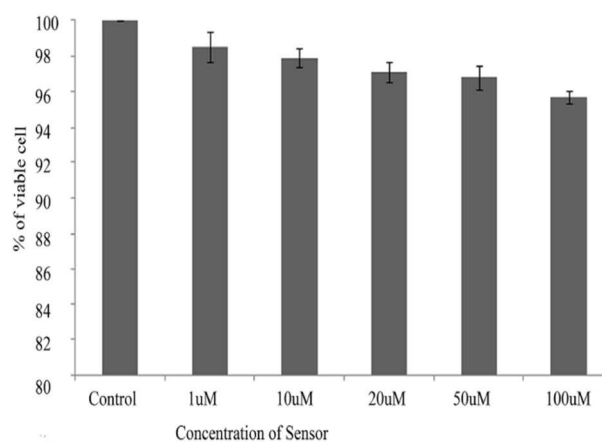
Fig. 11 represents % cell viability of A549 cells treated with different concentrations (1μM-100μM) of **PydDmen** for 12 h determined by MTT assay. Results are expressed as mean ± S.D of three independent ₅₅ experiments.

Conclusion

In conclusion, we have synthesized and characterized a new pyridoxal containing Schiff base turn-on Zn²⁺ probe, **PydDmen**. The poorly fluorescent probe responds giving a strong selective, ₆₀ fast and specific fluorescence signal in presence of Zn²⁺ ions, i.e. there is a zinc triggered fluorescence switching. The C=N isomerisation and ESIPT are inhibited upon binding with Zn²⁺ ions, which causes CHEF effect, inducing an enhancement in the fluorescence intensity of the chemosensor. The complex ₆₅ formation, stoichiometry, and binding mode have been thoroughly examined by UV–Vis, ESI-MS, and NMR studies, which show formation of an 1:1 **PydDmen-Zn²⁺** complex. The chelating agent EDTA can switch off the fluorescence signal by coordinating with the zinc ion, releasing the chemosensor to the solution. ^{1}H, ^{13}C ₇₀ NMR and DEPT analysis indicates Zn²⁺ induced transformation of the chemosensor to 3-pyridone tautomeric form. The DFT/TDDFT calculation was carried out to demonstrate the

electronic properties of the chemosensor and **PydDmen-Zn²⁺** and it supports the prevailing 3-pyridone tautomeric form. Furthermore, we have demonstrated that the probe is applicable for Zn²⁺ imaging in the living cells. We believe that the
5 development of a new turn-on Zn²⁺ probe, its outstanding fluorescence enhancement, spectroscopic and DFT studies, and cell imaging will find considerable application in the chemical science and its allied branches.

Experimental Section

10 **General information and materials**

All reagents were purchased from Sigma-Aldrich and used as received. Solvents were spectroscopic grade and used without purification. Elemental analyses (carbon, hydrogen and nitrogen) were carried out with a Perkin-Elmer CHN analyzer 2400. The ¹H
15 and ¹³C NMR spectra were measured on Bruker–300 MHz spectrometer. IR spectra were recorded in the region 400–4000 cm⁻¹ on a Bruker-Optics Alpha– T spectrophotometer with samples as KBr disks. Electronic spectra were obtained by using a Hitachi U-3501 spectrophotometer. Luminescence property was
20 measured using LS-55 Perkin Elmer fluorescence spectrophotometer at room temperature (298 K) by 1 cm path length quartz cell. Fluorescence lifetimes were obtained by the method of Time Correlated Single-Photon counting (TCSPC) on FluoroCube-01-NL spectrometer (Horiba Jobin Yvon) using a
25 nanoLED as light source (340 nm) and the signals were collected at the magic angle of 54.7° to eliminate any considerable contribution from fluorescence anisotropy decay. The typical time resolution of our experimental set up is 800 ps. The decays were deconvoluted using DAS-6 decay analysis software. The
30 acceptability of the fits was judged by χ^2 criteria (fitting analysis having χ^2 beyond the range $1.20 < \chi^2 < 1.00$ has been neglected) and visual inspection of the residuals of the fitted function to the data. Mean (average) fluorescence lifetimes were calculated using the following equation.

35 $<\tau_{av}> = \sum_i a_i \tau_i / \sum_i a_i$

in which a_i is the pre-exponential factor corresponding to the ith decay time constant, τ_i.

40 **Reagents for cell study**

A549, human lung cancer cell lines were collected from National Center for Cell Science, Pune, India, and used throughout the experiments. Cells were grown in DMEM (Himedia) supplemented with 10% FBS (Himedia), and an antibiotic mixture
45 (1%) containing PSN (Himedia) at 37ºC in a humidified incubator with 5% CO₂ and cells were grown to 80-90% confluence, harvested with 0.025% trypsin (Himedia) and in phosphate-buffered saline (PBS), plated at the desired cell concentration and allowed to grow overnight before any treatment.

50 **Imaging system**

Fluorescence images of A549 cells were taken by a fluorescence microscope (Model: LEICA DM4000B, Germany) with an objective lens of 20X magnification.

Cell culture

55 Cells were rinsed with PBS and incubated with DMEM containing **PydDmen** making the final concentration up to 10μM in DMEM [the stock solution (3 mmol) was prepared by dissolving **PydDmen** into ethanol] for 10 min at 37ºC. After incubation, bright field and fluorescence images of A549 cells
60 were taken by a fluorescence microscope (Model: LEICA DM4000B, Germany) with an objective lens of 20X magnification. Similarly, fluorescence images of A549 cells (pre-incubated with 10μM **PydDmen**) were taken with addition of different concentrations (1μM-50μM) of zinc nitrate salt at 10
65 minutes interval. A merged image between phase contrast and fluorescent images at 50μM salt concentration were taken and consequently fluorescence images were taken after further addition of TPEN (100μM).

Cell cytotoxicity assay

70 In order to test the cytotoxicity of **PydDmen**, 3-(4, 5-dimethylthiazol-2-yl)-2,S-diphenyltetrazolium bromide (MTT) assay was performed in A549 cells according to standard procedure.[30] Briefly, after treatment of overnight culture of A549 cells (10³ cells in each well of 96-well plate) with **PydDmen** (1,
75 10, 20, 50 and 100 μM) for 12 h, 10 μl of a MTT solution (1mg/ml in PBS) was added in each well and incubated at 37ºC continuously for 3 h. All media were removed from wells and 100μl of acidic isopropyl alcohol was added into each well. The intracellular formazan crystals (blue-violet) formed were
80 solubilized with 0.04N acidic isopropyl alcohol and absorbance of the solution was measured at 595 nm wavelength with a microplate reader (Model: THERMO MULTI SCAN EX). The cell viability was expressed as the optical density ratio of the treatment to control. Values are mean ± standard deviation of
85 three independent experiments. The cell cytotoxicity was calculated as % cell cytotoxicity = 100% - % cell viability.

Computational Studies

All geometries for **PydDmen** and **PydDmen-Zn²⁺** were optimized by density functional theory (DFT) calculations using Gaussian 09
90 (B3LYP/6-311G(d,p)) software package.[31] The vibrational frequency calculations were performed to ensure that the optimized geometries represent the local minima and that there is only positive eigen values. Vertical electronic excitations based on B3LYP optimized geometries were computed using the time-
95 dependent density functional theory (TDDFT) formalism[32] in ethanol using a conductor-like polarizable continuum model (CPCM).[33]

Fluorimetric analysis

Fluorescence quantum yields (Φ) were estimated by integrating
100 the area under the fluorescence curves with the following equation:

$\Phi_{sample} = (OD_{standard}/OD_{sample}) \times (A_{sample}/A_{standard}) \times \Phi_{standard}$

where, A is the area under the fluuorescence spectral curve and OD is the optical density of the compound at the excitation
105 wavelength. The standard used for the measurement of the fluorescence quantum yield was quinine sulphate (Φ = 0.54 in water).

Synthesis of the chemosensor PydDmen

The chemosensor molecule **PydDmen** was synthesized by

following procedure. Pyridoxal hydrochloride (0.406 g, 2 mmol) was dissolved in absolute ethanol (15 mL) in the presence of KOH (0.112 g, 2 mmol) with stirring. After 1 h of stirring, the separated white solid (KCl) was filtered and the obtained clear solution was added to a solution of N,N-dimethylethylenediamine (0.176g, 2 mmol) in ethanol (15 mL) with stirring and the resulting reaction mixture was refluxed for 4 h. The completeness of the condensation reaction was checked by performing thin layer chromatography. The solution was evaporated by rotary evaporator and sticky mass obtained was washed by cold ether and dried under vacuum. (Yield: 0.355g, 0.75%). ^{1}H NMR (300 MHz, DMSO-d$_6$): δ 8.797(s, H$_a$), 7.762(s, H$_d$), 4.548 (s, H$_b$), 3.672 (t, H$_g$), 2.471 (t, H$_h$), 2.271(s, H$_e$), 2.10 (s, H$_i$). Anal. calc. for C$_{12}$H$_{19}$N$_3$O$_2$: C, 60.74; H, 8.07; N, 17.71. Found: C, 59.97; H, 7.79; N, 17.05%.

Synthesis of PydDmen-Zn^{2+}

Pyridoxal hydrochloride (0.203g, 1 mmol) was dissolved in absolute ethanol. To it, ethanolic solution of Zn(NO$_3$)$_2$.2H$_2$O (0.297g, 1 mmol) was added dropwise under stirring and the solution was stirred for 15 min. Then to this solution, N,N-dimethylethylenediamine (0.088g, 1 mmol) was added slowly and the resulting yellowish-orange solution was stirred for 2 h. Then it was evaporated by rotary evaporator and resulting sticky mass was washed by cold ether and dried under vacuum. (Yield: 0.211g, 0.53%). Anal.calc. for [Zn(**PydDmen**)(NO$_3$)(H$_2$O)$_2$]: C, 36.06; H, 5.55; N,14.02. Found: C, 35.54; H, 5.14; N, 13.87%.

Acknowledgements

References

1 (a) A. I. Bush, W. H. Pettingell, G. Multhaup, M. Paradis, J. P. Vonsattel, J. F. Gusella, K. Beyreuther, C. L. Masters and R. E. Tanzi, *Science*, 1994, **265**, 1464–1465; (b) C. J. Frederickson, J. Y. Koh and A. I. Bush, *Nat. Rev. Neurosci.*, 2005, **6**, 449–452; (c) D. D. Mott, M. Benveniste and R. J. Dingledine, *J. Neurosci.*, 2008, **28**, 1659–1671; (d) J. M. Berg and Y. Shi, *Science*, 1996, **271**, 1081–1085.

2 A. Krężel and W. Maret, *J. Biol. Inorg. Chem.*, 2006, **11**, 1049-1062.

3 (a) A. I. Bush, *Trends Neurosci.*, 2003, 26, 207–214; (b) D. Noy, I. Solomonov, O. Sinkevich, T. Arad, K. Kjaer and I. Sagi, *J. Am. Chem. Soc.*, 2008, 130, 1376–1383; (c) C. V. Banks and R. E. Bisque, *Anal. Chem.*, 1957, 29, 522–526; (d) A. R. Fakhari, M. Shamsipur and K. H. Ghanbari, *Anal. Chim. Acta*, 2002, 460, 177–183; (e) Q. Li, X. H. Zhao, Q. Z. Lv and G. G. Liu, *Sep. Purif. Technol.*, 2007, **55**, 76–81.

4 (a) R. Y. Tsien, *Fluorescent and Photochemical Probes of Dynamic Biochemical Signals inside Living Cells*, ed. A. W. Czarnik, American Chemical Society, Washington, DC, 1993, 130–146; (b) Y. Xiang, A. J. Tong, P. Y. Jin and Y. Ju, *Org. Lett.*, 2006, **8**, 2863-2866.

5 (a) K. Kikuchi, K. Komatsu and T. Nagano, *Curr. Opin. Chem. Biol.*, 2004, **8**, 182–191; (b) E. L. Que, D. W. Domaille and C. J. Chang, *Chem. Rev.*, 2008, **108**, 1517–1549; (c) N. C. Lim, H. C. Freake and C. Bruckner, *Chem. Eur. J.*, 2005, **11**, 38–49; (d) Z. C. Xu, J. Y. Yoon and D. R. Spring, *Chem. Soc. Rev.*, 2010, **39**, 1996–2006.

6 (a) Y. H. Lau, P. J. Rutledge, M. Watkinson and M. H. Todd, *Chem. Soc. Rev.*, 2011, **40**, 2848-2866; (b) D. Maity and T. Govindaraju, *Chem. Commun.*, 2010, **46**, 4499-4501; (c) K. Jobe, C. H. Brennan, M. Motevalli, S. M. Goldup and M. Wakinson, *Chem. Commun.*, 2011, **47**, 6036-6038; (d) T. L. Mindt, H. Struthers, L. Brans, T. Anguelov, C. Schweinsberg, V. Maes, D. Tourwe and B. Schibli, *J. Am. Chem. Soc.*, 2006, **128**, 15096-15097; (e) C. Ornelas, J. R. Aranzaes, E. Cloutet, S. Alves and D. Astruc, *Angew. Chem., Int. Ed.*, 2007, **46**, 872-877; (f) K. -C. Chang, I. -H. Su, A. Senthilvelan and W. -S. Chung, *Org. Lett.*, 2007, **9**, 3363-3366; (g) B. Colasson, M. Save, P. Milko, J. Roithova, D. Schroder and O. Reinaud, *Org. Lett.*, 2007, **9**, 4987-4990; (h) S. Huang, R. J. Clark and L. Zhu, *Org. Lett.*, 2007, **9**, 4999-5002; (i) K. -C. Chang, I. -H. Su, G. -H. Lee and W.-S. Chung, *Tetrahedron Lett.*, 2007, **48**, 7274-7278; (j) R. M. Meudtner, M. Ostermeier, R. Goddard, C. Limberg and S. Hecht, *Chem. Eur. J.*, 2007, **13**, 9834-9840; (k) S. Y. Park, J. H. Yoon, C. S. Hong, R. Souane, J. S. Kim, S. E. Matthews and J. Vicens, *J. Org. Chem.*, 2008, **73**, 8212-8218; (l) D. Schweinfurth, K. I. Hardcastle and U. H. F. Bunz, *Chem. Commun.*, 2008, 2203-2205; (m) M. Juricek, P. H. J. Kouwer, J. Rehak, J. Sly and A. E. Rowan, *J. Org. Chem.*, 2009, **74**, 21-25; (n) J. Camponovo, J. Ruiz, E. Cloutet and D. Astruc, *Chem. Eur. J.*, 2009, **15**, 2990-3002; (o) R. K. Pathak, V. K. Hinge, M. Mondal and C. P. Rao, *J. Org. Chem.*, 2011, **76**, 10039-10049.

7 (a) K. K. Upadhyay, A. Kumar, J. Zhao and R. K. Mishra, *Talanta*, 2010, **81**, 714–721; (b) J. F. Zhang, S. Kim, J. H. Han, S. J. Lee and J. S. Kim, *Org. Lett.*, 2011, **13**, 5294–5297; (c) Y. Xu, J. Meng, L. X. Meng, Y. Dong, Y. X. Cheng and C. J. Zhu, *Chem. Eur. J.*, 2010, **16**, 12898–12903; (d) Q. H. You, P. S. Chan, W. H. Chan, N. K. Mak and R. N. S. Wong, *RSC Adv.*, 2012, **2**, 11078–11083; (e) H. Y. Lin, P. Y. Cheng, C. F. Wan and A. T. Wu, *Analyst*, 2012, **137**, 4415–4417.

8 (a) S. Comby, S. A. Tuck, L. K. Truman, O. Kotova and T. Gunnlaugsson, *Inorg. Chem.*, 2012, **51**, 10158–10168; (b) J. Jia, Q. C. Xu, R. C. Li, X. Tang, Y. F. He, M. Y. Zhang, Y. Zhang and G. W. Xing, *Org. Biomol. Chem.*, 2012, **10**, 6279–6286; (c) X. Meng, S. Wang, Y. Li, M. Zhu and Q. Guo, *Chem. Commun.*, 2012, **48**, 4196–4198; (d) T. Mukherjee, J. C. Pessoa, A. Kumar and A. R. Sarkar, *Dalton Trans.*, 2012, **41**, 5260–5271; (e) S. H. Mashraqui, R. Betkar, S. Ghorpade, S. Tripathi and S. Britto, *Sens. Actuators, B*, 2012, **174**, 299–305.

9 (a) G. Mandal, M. Darragh, Y. A. Wang and C. D. Heyes, *Chem. Commun.*, 2013, **49**, 624–626; (b) G. Sivaraman, T. Anand and D. Chellappa, *Analyst*, 2012, **137**, 5881–5884; (c) L. J. Liang, S. J. Zhen, X. J. Zhao and C. Z. Huang, *Analyst*, 2012, **137**, 5291–5294; (d) P. G. Sutariya, N. R. Modi, A. Pandya, B. K. Joshi, K. V. Joshi and S. K. Menon, *Analyst*, 2012, **137**, 5491–5494; (e) Y. W. Choi, G. J. Park, Y. J. Na, H. Y. Jo, S. A. Lee, G. R. You and C. Kim, *Sens. Actuators, B*, 2014, **194**, 343–352; (f) E. J. Song, H. Kim, I. H. Hwang, K. B. Kim, A. R. Kim, I. Noh and C. Kim, *Sens. Actuators, B*, 2014, **195**, 36–43; (g) G. J. Park, H. Kim, J. J. Lee, Y. S. Kim, S. Y. Lee, S. Lee, I. Noh, C. Kim, *Sens. Actuators, B*, 2015, **215**, 568–576; (h) J. J. Lee, S. A. Lee, H. Kim, L. T. Nguyen, Insup Noh and Cheal Kim, *RSC Adv.*, 2015, **5**, 41905-41913; (i) A. K. Bhanja, C. Patra, S. Mondal, D. Ojha, D. Chattopadhyay and C. Sinha, *RSC Adv.*, 2015, **5**, 48997-49005; (j) C.-X. Yin, L.-J. Qu, F.-J. Huo, *Chin. Chem. Lett.*, 2014, **25**, 1230–1234.

10 J. Wu, W. Liu, X. Zhuang, F. Wang, P. Wang, S. Tao, X. Zhang, S. Wu and S. T. Lee, *Org. Lett.*, 2007, **9**, 33–36.

11 (a) X. Zhang, L. Guo, F. Y. Wu and Y. B. Jiang, *Org. Lett.*, 2003, **5**, 2667–2670; (b) M. Royzen, A. Durandin, V. G. Young, N. E. Geacintov and J. W. Canary, *J. Am. Chem. Soc.*, 2006, **128**, 3854-3855.

12 (a) Z. Xu, K. -H. Baek, H. N. Kim, J. Cui, X-Qian, D. R. Spring, I. Shin and J. Yoon, *J. Am. Chem. Soc.*, 2010, **132**, 601-610; (b) Z. Xu, X. Liu, J. Pan and D. R. Spring, *Chem. Commun.*, 2012, **48**, 4764 - 4766.

13 (a) V. Bhalla, Roopa and M. Kumar, *Dalton Trans.*, 2013, **42**, 975-980; (b) V. Bhalla, Roopa and Manoj Kumar, *Org. Lett.*, 2012, **14**, 2802-2805; (c) A. Satheshkumar, E. H. El-Mossalamy, R. Manivannan, C. Parthiban, L. M. Al-Harbi, S. Kosa and K. P. Elango, *Spectrochim. Acta, Part A*, 2014, **128**, 798-805; (d) M. J. Kim, K. Kaur, N. Singh and D. O. Jang, *Tetrahedron*, 2012, **68**, 5429-5433; (e) K. Kaur, V. K. Bhardwaj, N. Kaur and N. Singh, *Inorg. Chem. Commun.*, 2012, **26**, 31–36 (f) B. Babur, N. Seferogˇlu and Z. Seferogˇlu, *Tetrahedron Lett.*, 2015, **56**, 2149–2154; (g) A. D. Dubonosov, V. I. Minkin, V. A. Bren, E. N. Shepelenko, A. V. Tsukanov, A. G. Starikov, G. S. Borodkin, *Tetrahedron*, 2008, **64**, 3160-3167; (h) A. Misra and M. Shahid, *J. Phys. Chem. C*, 2010, **114**, 16726–16739; (i) S. Mukherjee, A. K. Paul and H. S.-Evans, *Sensors and Actuators, B*, 2014, **202**, 1190–1199; (j) A. Samanta, S. Dalapati and N. Guchhait, *J. Photochem. Photobiol. A*, 2012, **232,** 64–72; (k) Z. -H. Pan, J. -W. Zhou and G. -G. Luo, *Phys. Chem. Chem. Phys.*, 2014, **16**, 16290-16301; (l) B. Liu, H. Wang, T. Wang, Y. Bao, F. Du, J. Tian, Q. Li and R. Bai, *Chem. Commun.*, 2012, **48**, 2867–2869.

14 S. Mandal, R. Modak and S. Goswami, *J. Mol. Struct.*, 2013, **1037**, 352-360.

15 T. Mukherjee, J. C. Pessoa, A. Kumar and A. R. Sarkar, *Dalton Trans.*, 2012, **41**, 5260–5271.

16 A. C. Eliot and J. F. Kirsch, *Annu. Rev. Biochem.*, 2004, **73**, 383-415.

17 R. A. John, *Biochim. Biophys. Acta*, 1995, **1248**, 81-96.

18 M. D. Toney, *Arch. Biochem. Biophys.*, 2005, **433**, 279-287.

19 P. Christen and D. E. Metzler, *Transaminases*, Wiley, New York. 1985.

20 H. Hayashi, H. Mizuguchi, I. Miyahara, M. M. Islam, H. Ikushiro, Y. Nakajima, K. Hirotsu, H. Kagamiyama, *Biochim. Biophys. Acta*, 2003, **1647**, 103-109.

21 W. Liu, P. E. Peterson, J. A. Langston, X. Jin, X. Zhou, A. J. Fisher and M. D. Toney, *Biochemistry,* 2005, **44**, 2982-2992.

22 O. K. Abou-Ziad and O. I. K. Al-Shini, *Phys. Chem. Chem. Phys.*, 2009, **11**, 5377–5383.

23 K. Nakamoto, *Infrared Spectra of Inorganic Compounds*, Wiley, New York, 1970.

24 L. Wang, W. Qin, X. Tang, W. Dou and W. Liu, *J. Phys. Chem. A*, 2011, **115**, 1609–1616.

25 (a) L. Long, D. Zhang, X. Li, J. Zhang, C. Zhang and L. Zhou, *Anal. Chim. Acta,* 2013, **775***,* 100–105; (b) M. Zhu, M. Yuan, X. Liu, J. Xu, J. Lv, C. Huang, H. Liu, Y. Li, S. Wang and D. Zhu, *Org. Lett.,* 2008, **10**, 1481-1484; (c) C. Kar, M. D. Adhikari, A. Ramesh and G. Das, *Inorg. Chem.,* 2013, **52**, 743−752.

26 G. L. Long and J. D. Winefordner, *Anal. Chem.*, 1983, **55**, 712A-724A.

27 B. K. Paul, S. Kar and N. Guchhait, *J. Photochem. Photobiol. A*, 2011, **220**, 153−163.

28 B. Valeur, *Molecular Fluorescence: Principles and Applications*, Wiley-VCH, Weinheim, Germany, 2002.

29 (a) A. D. Becke, *J. Chem. Phys.,*1993, **98**, 5648-5652; (b) C. Lee, W. Yang and R. G. Parr, *Phys. Rev. B*, 1988, **37**, 785-789.

30 T. Mossman, *J. Immunol. Methods,* 1983, **65**, 55-63.

31 M. J. Frisch, G. W. Trucks, H. B. Schlegel, G. E. Scuseria, M. A. Robb, J. R. Cheeseman, G. Scalmani, V. Barone, B. Mennucci, G. A. Petersson, H. Nakatsuji, M. Caricato, X. Li, H. P. Hratchian, A. F. Izmaylov, J. Bloino, G. Zheng, J. L. Sonnenberg, M. Hada, M. Ehara, K. Toyota, R. Fukuda, J. Hasegawa, M. Ishida, T. Nakajima, Y. Honda, O. Kitao, H. Nakai, T. Vreven, J. A. Montgomery, Jr., J. E. Peralta, F. Ogliaro, M. Bearpark, J. J. Heyd, E. Brothers, K. N. Kudin, V. N. Staroverov, R. Kobayashi, J. Normand, K. Raghavachari, A. Rendell, J. C. Burant, S. S. Iyengar, J. Tomasi, M. Cossi, N. Rega, J. M. Millam, M. Klene, J. E. Knox, J. B. Cross, V. Bakken, C. Adamo, J. Jaramillo, R. Gomperts, R. E. Stratmann, O. Yazyev, A. J. Austin, R. Cammi, C. Pomelli, J. W. Ochterski, R. L. Martin, K. Morokuma, V. G. Zakrzewski, G. A. Voth, P. Salvador, J. J. Dannenberg, S. Dapprich, A. D. Daniels, Ö. Farkas, J. B. Foresman, J. V. Ortiz, J. Cioslowski, and D. J. Fox, Gaussian 09, Revision D.01, Gaussian, Inc., Wallingford CT, 2009.

32 (a) R. Bauernschmitt and R. Ahlrichs, *Chem. Phys. Lett.,* 1996, **256**, 454-464; (b) R. E. Stratmann, G. E. Scuseria and M. J. Frisch, *J.*

Chem. Phys., 1998, **109**, 8218-8224; (c) M. E. Casida, C. Jamorski, K. C. Casida, D. R. Salahub, *J. Chem. Phys.,* 1998, **108**, 4439-4449.

33 (a) V. Barone and M. Cossi, *J. Phys. Chem. A*, 1998, **102**, 1995-2001; (b) M. Cossi and V. Barone, *J. Chem. Phys.*, 2001, **115**, 4708-4717; (c) M. Cossi, N. Rega, G. Scalmani and V. Barone, *J. Comput. Chem.*, 2003, **24**, 669-681.

A new pyridoxal based fluorescence chemo-sensor for detection of Zn(II) and its application in bio imaging †

Senjuti Mandal,[a] **Yeasin Sikdar,**[a] **Dilip K. Maiti,**[a] **Guru Prasad Maiti,**[b] **Sushil Kumar Mandal,**[c] **Jayanta Kumar Biswas,**[c] **Sanchita Goswami**[a*]
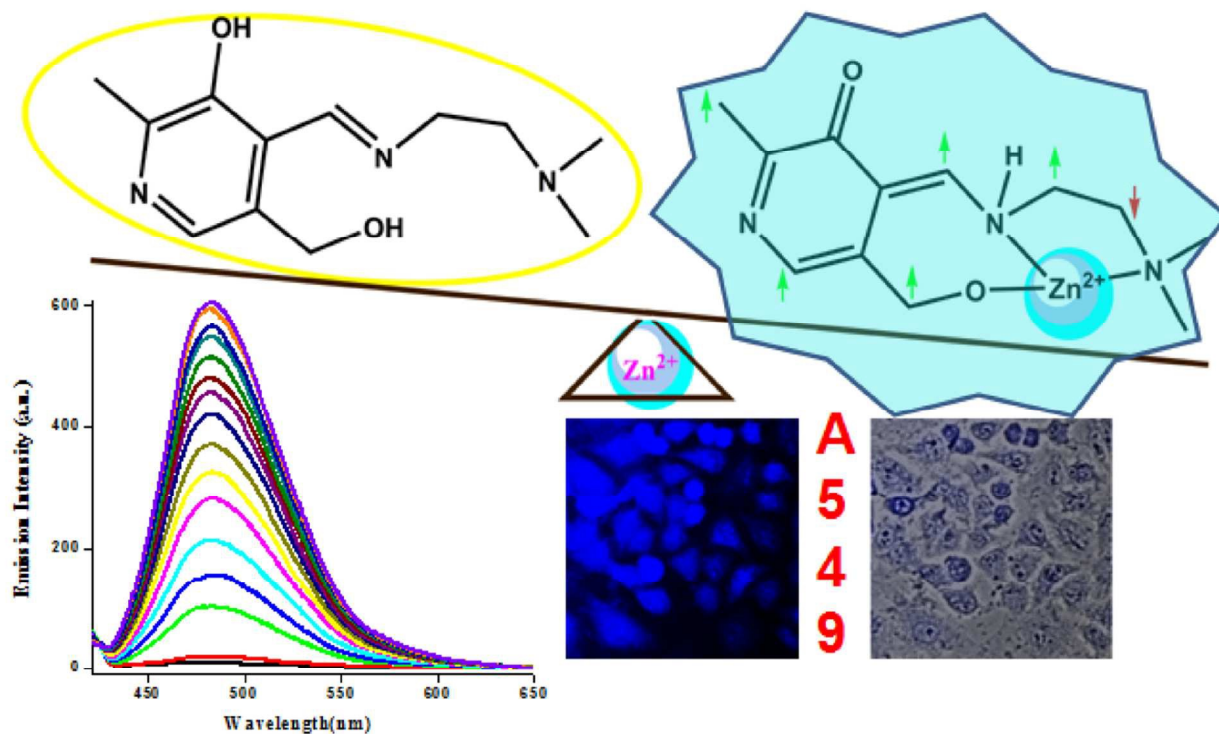
A new pyridoxal-based reversible chemosensor was synthesized that exhibits selective turn-on type response in presence of Zn^{2+} in ethanol – water mixture. The experimental and theoretical supports in terms NMR spectroscopy and DFT are provided to establish the existence of Zn^{2+} induced transformation of **PydDmen** to a 3-pyridone tautomeric form.